$Z(3)$ criticality in three dimensions: Study of extended Potts models

R. V. Gavai
Tata Institute of Fundamental Research, Homi Bhabha Road, Bombay 400 005, India

F. Karsch
Höchstleistungsrechenzentrum (HLRZ), c/o Forschungszentrum Jülich, P.O. Box 1913, D-5170 Jülich, Germany and Fakultät für Physik, Universität Bielefeld, D-4800 Bielefeld 1, Germany

(Received 20 May 1991; revised manuscript received 5 November 1991)

We investigate numerically the three-dimensional three-state Potts models with nearest-neighbor (NN) ferromagnetic coupling and next-nearest-neighbor (NNN) antiferromagnetic coupling of relative strength γ on L^3 lattices with $L=12$, 16, 20, 32, and 40. For all the γ values that we studied, $0.0 \leq \gamma \leq 0.8$, we find indications of a first-order phase transition between the ordered and disordered phases. In the neighborhood of $\gamma=0.25$, the latent heat becomes rather small, making it necessary to use still larger lattices to rule out a higher-order phase transition at $\gamma=0.25$. We also studied the boundary regimes of the three different ordered phases and find no criticality along them, thus suggesting a lack of criticality in these extended Potts models.

I. INTRODUCTION

The investigation of spin models has proved to be a fruitful area of research for both condensed-matter and particle physics. Recently, the old issue of the nature of phase transitions in various $Z(3)$ spin models in three dimensions[1] has again come into the limelight because of some surprising results of Bacielieri *et al.*[2] on the order of the deconfinement phase transition in SU(3) gauge theory. While early numerical simulations[3] indicated a first-order phase transition, the results of Bacielieri *et al.* suggested[4] a second-order deconfinement phase transition. This led to a thorough reexamination of some basic assumptions underlying the universality arguments,[5] which predict that the phase transition in SU(3) gauge theory a finite temperature should be first order.

An essential ingredient of such an argument is the assumption of a lack of $Z(3)$ criticality. The numerical simulations of three-dimensional $Z(3)$-symmetric spin models therefore witnessed a natural rekindling of interest. Of particular importance in this context is the question of the order of the phase transition between ordered and disordered phases of a model with nearest neighbor (NN) ferromagnetic and arbitrary next-to-nearest neighbor (NNN) interactions. If a continuous transition were to be found for such a model, then it will be of tremendous interest for both the condensed-matter and particle physics to understand its origin. It will further suggest a possibility that the results obtained for the SU(3) gauge theory so far may change even qualitatively on larger lattices which are necessary to remove eventually the space-time lattice and obtain a continuum field theory.

The NN ferromagnetic Potts model with antiferromagnetic NNN interactions of relative strength γ is also interesting as a simple model for spin glasses. In three dimensions the model is expected to have degenerate ground states for $\gamma > 0.25$. In fact, the model exhibits a rich phase structure and has two additional ordered phases. These have[6] ferromagnetic ordering only in planes and lines and thus break translational invariance in one and two directions, respectively. The different antiferromagnetic orderings of the planes and lines give rise to the degeneracy of the ground states in these phases. Nothing seems to be known about the nature of the phase transition separating the different ordered phases. Previous simulations[6] have explored the phase diagram and found deviations from naive expectations, but the model deserves a more detailed numerical exploration.

The model has been recently investigated in high-statistics simulations for $0 \leq \gamma \leq 0.2$.[7,8] These studies showed no evidence for critical behavior; in all cases, a first-order phase transition has been found. In this paper we extend our earlier work on the three-dimensional three-state Potts model[7,9] with $\gamma=0.0$ and 0.2 and investigate in detail the order-disorder phase transition in the entire positive-γ regime. In the next section, we define the model and observables we study along with the details of our methods. Section III contains our results on the phase diagram of the model, and in the final section we present our conclusions.

II. MODEL

The Hamiltonian for the three-dimensional three-state Potts model with a relative strength of the antiferromagnetic NNN coupling γ is given by

$$H=-\left[\sum_{\substack{\text{NN pairs}\\ \langle j,k\rangle}} \delta_{\sigma_j,\sigma_k} - \gamma \sum_{\substack{\text{NNN pairs}\\ \langle j,k\rangle}} \delta_{\sigma_j,\sigma_k}\right], \tag{1}$$

where $\sigma_j,\sigma_k=0,1,2$ define the spin on a site j or k of a three-dimensional lattice L^3:

$$P_j = \exp(2\pi i \sigma_j/3) \ . \tag{2}$$

The corresponding partition function is given by[10]

$$Z = \sum_{\{\sigma_j\}} \exp(-\beta H) \ . \tag{3}$$

The antiferromagnetic coupling γ ($\gamma > 0$) introduces competing interactions and hence frustrations, since it favors nonalignment of next-to-nearest neighbor spins. Of course, for very small γ, one still expects the system to show ferromagnetic ordering. As γ increases, however, other orderings become energetically more favorable. Noting that in three dimensions one has two nearest neighbors but eight next-to-nearest neighbors out of a plane, one sees that, for $2-8\gamma<0$ or $\gamma>\frac{1}{4}$, one will achieve lower energy by having stacks of ferromagnetically ordered planes, but with neighboring planes residing in different $Z(3)$ states: $\sigma_i \neq \sigma_j$, $\forall i = j \pm 1$, where i and j denote planes orthogonal to a given direction. As γ increases, a further loss of ferromagnetic ordering becomes energetically favorable: Replacing each alternate column of spins by σ_k in a ferromagnetically ordered plane with spins $\sigma_i \neq \sigma_k$ causes an energy change $2-4\gamma$, which becomes negative for $\gamma > \frac{1}{2}$. It is clear from the above arguments that entropy of the ground state becomes proportional to (i) L in the type-I superantiferromagnetic (SAF I) phase, corresponding to $\frac{1}{4} < \gamma < \frac{1}{2}$, and (ii) L^2 in the type-II superantiferromagnetic (SAF II) phase, corresponding to $\gamma > \frac{1}{2}$. In Fig. 1 we show typical configurations from runs in the four different phases of the model, which have been taken from simulations of 12^3 lattices. The progressive loss of ferromagnetic ordering is clearly visible in them.

Based on the classical considerations of the minimization of energy discussed above, one obtains the horizontal lines at $\gamma = 0.25$ and 0.5 in the phase diagram of the model, shown in Fig. 2. The vertical lines in the phase diagram correspond to expected disorder-order phase boundaries. For $\gamma < 0.25$ a standard leading-order mean-field approximation leads to the following prediction for the disorder-order phase transition: $\beta_c = 0.4621/(1-2\gamma)$. For larger values of γ, the anticipated lack of full translational invariance of the ground state complicates the mean-field analysis. Intuitively, some crude guesses can be made by considering two simple extremes, which are shown in Fig. 2 by a dashed and a solid vertical line. Noting that the ferromagnetic ordering persists in planes in the SAF I phase and in lines in SAF II phase, respectively, one can exploit the mean-field predictions for two- and one-dimensional models with ferromagnetic NN coupling and antiferromagnetic NNN coupling. They are, respectively, $\beta_c = 0.6932/(1-\gamma)$ and $\beta_c = 1.3863$. One may use them as first guesses for the full three-

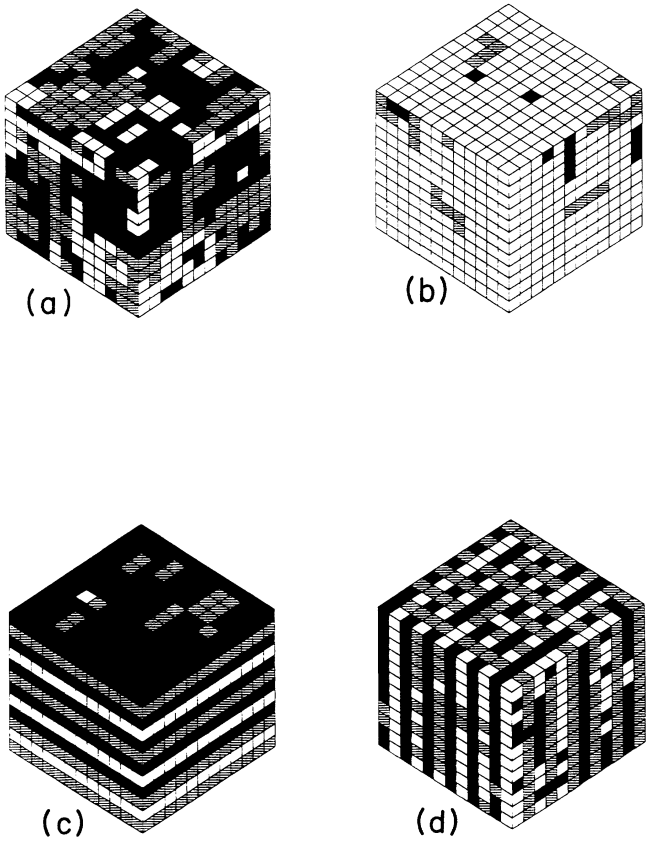

FIG. 1. Examples of typical configurations on a 12^3 lattice in the (a) disordered, (b) ferromagnetic, (c) type-I and (d) type-II superantiferromagnetic phases. The couplings used in these specific runs are (β,γ)= (a) (1.805,0.255), (b) (1.645,0.24), (c) (1.807,0.255), and (d) (1.7,0.57).

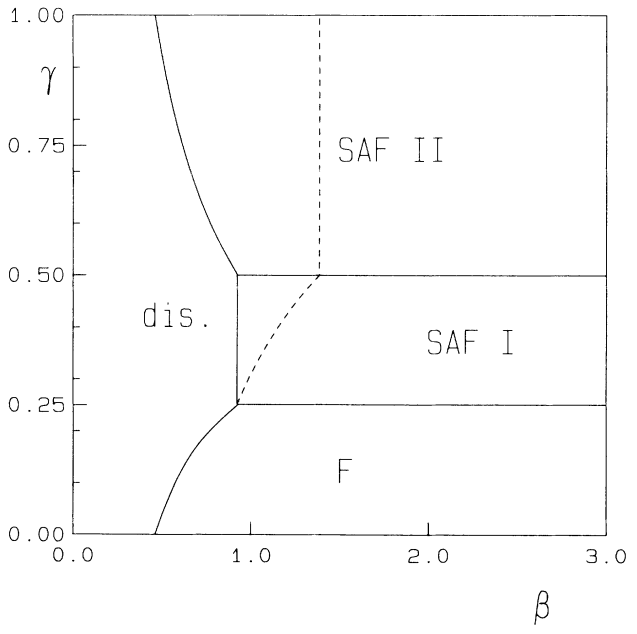

FIG. 2. Expected phase diagram of the NNN Potts model with antiferromagnetic coupling in the (β,γ) plane. The horizontal lines are from classical minimum-energy considerations, while the other lines are explained in the text.

dimensional model for $0.25<\gamma<0.5$ and for $\gamma>0.5$, respectively. The dashed line in Fig. 2 represents these predictions. Alternatively, one can treat the model in these two regions as effective antiferromagnetic models.[6] The assembly of ferromagnetically ordered planes in the region $0.25<\gamma<0.5$ can be thought of as a one-dimensional system of spins with antiferromagnetic NN coupling. Similarly, considering the ferromagnetically ordered lines for $\gamma>0.5$ as individual spins, one arrives at a two-dimensional antiferromagnetic spin model. The solid line for $\gamma>0.25$ in Fig. 2 shows the predictions.

Note, however, that both sets of predictions should be regarded as elementary guesses in view of the drastic approximations involved in arriving at them. The aim of this paper is to explore the phase diagram numerically to find out where the phase boundaries lies and what their nature is.

The observables which we investigated are the energy density $\langle \varepsilon \rangle$, given by

$$\langle \varepsilon \rangle = \langle H/V \rangle = 3[C_{\mathrm{NN}} - 2\gamma C_{\mathrm{NNN}}] . \tag{4}$$

Here $C_{\mathrm{NN}} = (3L^3)^{-1} \langle \sum_{\mathrm{NN}} \delta_{\sigma_j,\sigma_k} \rangle$ denotes the nearest-neighbor link expectation value and C_{NNN} accordingly gives the next-nearest-neighbor link expectation value. The order parameter $\langle S \rangle$ is defined by

$$S = \frac{3}{2L^3} \max(n_0, n_1, n_2) - \frac{1}{2} , \tag{5}$$

where n_α denotes the number of spins having value $\alpha = 0, 1, 2$. Note that $S=0$ for a random or disordered state and $S=1$ for a ferromagnetically ordered state. Further, both the superantiferromagnetic phases also have vanishingly small S. In order to distinguish the superantiferromagnetic phases from the disordered one, we also considered additional observables which were designed to probe for the violation of translational invariance. For a given direction $\hat{\mu}$ of the lattice, $\mu = 1, 2, 3$, we define S_μ as the spin order parameter on a plane perpendicular to $\hat{\mu}$ and average it over all such planes for a given configuration:

$$S_\mu = \frac{1}{L} \sum_{j=1}^{L} \left[\frac{3}{2L^2} \max(n_0^j, n_1^j, n_2^j) - \frac{1}{2} \right] , \tag{6}$$

where n_α^j are the same as n_α above, but for the jth plane perpendicular to $\hat{\mu}$. From the discussion of various phases above, it is easy to deduce that $S_1 = S_2 = S_3 = S$ for a ferromagnetically ordered and a disordered state. The value of S distinguishes between the two. The observables S_μ are useful in distinguishing the superantiferromagnetic states. For the SAF I phase, $\langle S_1 \rangle > \langle S_2 \rangle = \langle S_3 \rangle$, while for the SAF II phase, $\langle S_1 \rangle = \langle S_2 \rangle > \langle S_3 \rangle$. Of course, S_μ will have large finite-size effects, being typically $O(1/L^2)$, and hence verifications of the above relations may need large lattices. On smaller lattices and/or couplings close to the order-disorder line, there will also be flips causing a change of direction in which translational invariance is broken. A sufficient number of such flips may wash out some asymmetries. This behavior is very similar to the elementary spin order parameter $S_{\mathrm{elem}} = \sum_{i=1}^{L^3} P_i / L^3$, with P_i defined in Eq. (2). As is well known, S_{elem} is zero even at high temperatures in a finite volume because of its equal probability in the three $Z(3)$ vacua and tunnelings in a finite volume. Motivated by the usual modification of S_{elem} to overcome this problem, given in Eq. (5), one can also modify the S_μ's appropriately:

$$\begin{aligned} \bar{S}_1 &= \max(S_1, S_2, S_3) , \\ \bar{S}_2 &= \max(\min(S_1, S_2), \min(S_1, S_3)) , \\ \bar{S}_3 &= \min(S_1, S_2, S_3) . \end{aligned} \tag{7}$$

Thermal expectation values of $\bar{S}_\mu$'s over a chain of configurations can now be used to check for the relations for S_μ's above. Alternatively, one can study the time histories of S_μ to disentangle the flips.

In our Monte Carlo (MC) simulations, we used a standard Metropolis algorithm to simulate the model on periodic cubic lattices of linear sizes $L = 12$, 16, 20, 24, 32, 40, and 48. As we explain below, for some pairs of (β, γ) only, a subset of these was used. The observables were measured every tenth iteration to reduce autocorrelations. Standard methods were used to attempt a further reduction of the autocorrelations. At each pair of (β, γ) and on each lattice size, typically 500 000 to a few times 10^6 iterations were performed. In the next section, results of our explorations of the phase diagram are presented in detail.

III. RESULTS

A. Ferromagnetic phase: $0 \le \gamma \le 0.25$

As can be seen from Fig. 2, this region of the coupling space is expected to be a straightforward extension of the familiar NN Potts model, with a transition line separating the disordered and ferromagnetic phases. One hopes to confirm this with the help of numerical simulations. In particular, one wants (i) to find out the nature of the phase transition along the order-disorder line and (ii) to explore the nature of the phase boundary between the ferromagnetic and superantiferromagnetic phases. We have already presented our results for $\gamma = 0.0$ and 0.2 in Refs. 7 and 9, respectively. We will therefore present here only our additional results, after recalling briefly our main findings from Refs. 7 and 9 in order to justify our methodology, which we continue to employ here also. There have also been other numerical simulations[8] for $\gamma = 0.0$, 0.1, and 0.2. We will compare our results with them whenever possible.

Figure 3 displays our results for $\langle S \rangle$ as a function of β for $\gamma = 0.0$ and lattices of sizes $L = 12$, 20, 24, 30, 36, and 48. The increase of the sharpness of the crossover between the ordered and disordered phases with increasing volume is suggestive of a discontinuity in $\langle S \rangle$ in the infinite volume. Another qualitative indication of the first-order nature of the transition comes from an inspection of the Monte Carlo time evolution of the order parameter, shown in a typical example in Fig. 4 for the 36^3

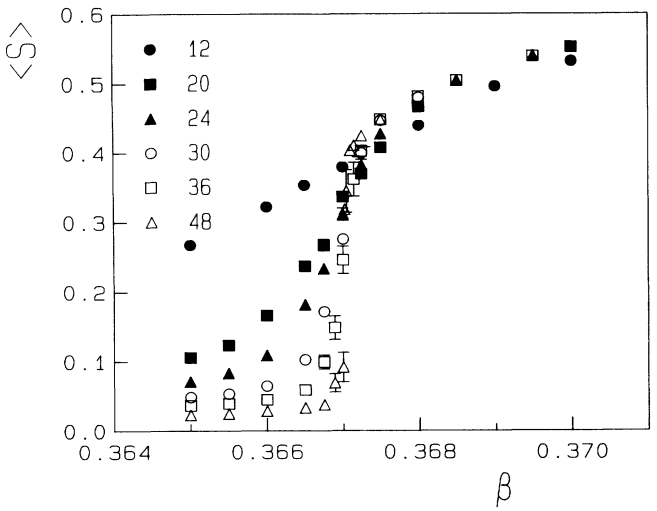

FIG. 3. Spin order parameter $\langle S \rangle$ as a function of β at $\gamma=0.0$ on L^3 lattices for $L=12$, 20, 24, 30, 36, and 48.

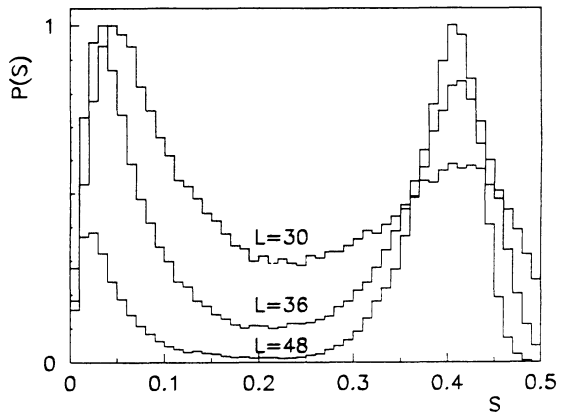

FIG. 5. Probability distributions of the order parameter S in the critical region of 30^3, 36^3, and 48^3 lattices at $(\beta,\gamma)=(0.5505,0.0)$.

lattice in its critical region: The system shows a clear flip-flop between two well-separated states. Of course, one needs to exercise caution in drawing conclusions from such a behavior, as demonstrated by some dramatic examples in Ref. 11. Indeed, one needs to supplement the above evidences by a finite-size scaling analysis to be more confident about the findings, especially if the discontinuity in the order parameter is rather small. Figure 5 shows the probability distributions of the order parameter S for 30^3, 36^3, and 48^3 lattices in the critical region. Again, the qualitative features here are suggestive of a first-order phase transition: One has a well-separated two-peak structure in which the overlap of the peaks decreases, and they move away from each other, if at all, as the volume increases. One can exploit the information contained in such histograms to obtain a precise value of $\beta_{c,L}$ and σ_L, where $\beta_{c,L}$ denotes inverse critical temperature for a lattice of size L and σ_L is the width of the corresponding critical region. This was done in Ref. 9, and

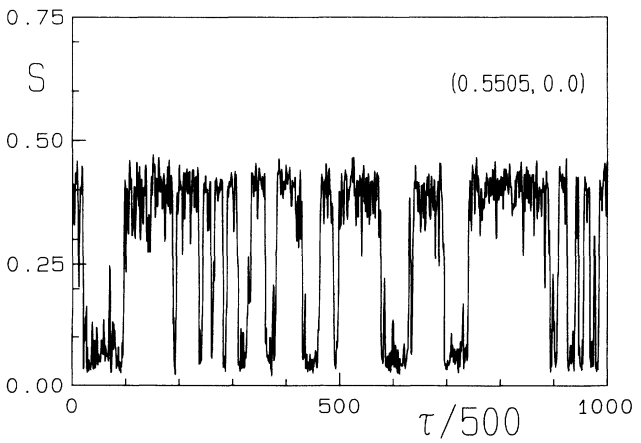

FIG. 4. Time evolution of the average spin S on a 36^3 lattice at $(\beta,\gamma)=(0.5505,0.0)$.

one found that both $\beta_{c,L}$ and σ_L exhibited a V^{-1} scaling behavior in accord with the expectations from a finite-size scaling behavior of a (discontinuity-fixed point-governed) first-order phase transition. It has been further shown by Fukugita *et al.*[8] that the widths of the critical region extracted from the specific heat and magnetic susceptibility also scale as V^{-1} and the corresponding maxima scale as volume. For $\gamma=0.0$ they obtained $\beta_{c,\infty}=0.550\,55(5)$, while Ref. 9 obtained $\beta_{c,\infty}=0.550\,62(3)$.

Because of the work of Ref. 2, the subject of correlation lengths in a model with a first-order phase transition acquired a lot of interest and was investigated in considerable detail for the $\gamma=0.0$ case in Refs. 8 and 9. The main results, which motivated us not to consider correlation length as a tool to find out the nature of the transition, are summarized below. The tunneling correlation length, which owes its presence to degenerate vacua, makes the extraction of the physical correlation length both complex and ambiguous in the critical region. This, in turn, renders a determination of the corresponding critical index untrustworthy. While a variety of prescriptions can be formulated to eliminate the tunneling correlation length, they result in a systematic error of unknown size for the physical correlation length. This makes it difficult to be sure whether the latter has a discontinuity or a cusp in the infinite-volume limit, although $\xi_{\rm phys}\sim 10$ is indicated for $\gamma=0.0$. We refer the interested reader to Refs. 8 and 9 for further details. It may be remarked here that attempts have been made in the literature to use the raw data on correlation length (i.e., containing the tunneling correlation length) to obtain information on the order of the phase transition. We feel, however, that even these were based on subjective and rather imprecise criteria.

Figure 6 exhibits $\langle S \rangle$ as a function of β for $\gamma=0.2$ on cubic lattices of size $L=20$, 24, 32, 40, and 48. These results are essentially the same as those presented in Ref. 7 except for the 32^3 lattice. Our new results are shifted in β by ~ 0.001 and thus suggest a lot smoother behavior of $\beta_{c,L}$ as a function of L. The only difference between the

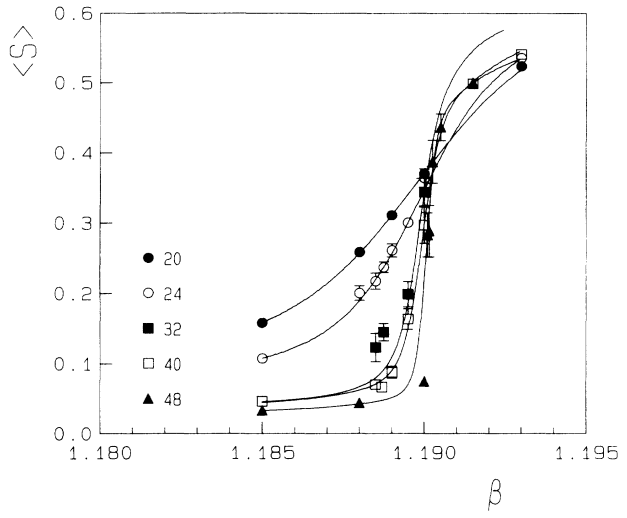

FIG. 6. Spin order parameter $\langle S \rangle$ as a function of β at $\gamma=0.2$ on L^3 lattices for $L=20$, 24, 32, 40, and 48.

two sets of results is in the random numbers.[12] Instead of drawing $2L^3$ random numbers per iteration, as done in Ref. 7, we generated p random numbers for every iteration, where p is the smallest prime number which is greater than $2L^3$, and discarded the last $p-2L^3$. While there are reasons to believe that spurious correlations with a period 2^n, n large, may exist in the usual random-number generators (in our case, RANF on a Cray supercomputer), making $L=32$ a special case,[13] these results are also a reminder that one needs to check the dependence of the physical results on the random numbers by varying the random-number generators. Indeed, we employed yet another random-number generator which even uses a subtractive algorithm,[14] unlike the multiplicative one in RANF, and confirmed that it too yielded the same β_c. Fortunately, no qualitative and very little quantitative change seems to occur as a result of the spurious correlations in RANF. In particular, finite-size scaling appears to set still for $L \geq 32$, as compared with $L \geq 20$ for $\gamma=0.0$, and the first-order nature of the transition remains unaltered, as extensive finite-size scaling studies[7,8] of various physical observables have shown. Results for the critical couplings are, however, now in much better agreement with results of Billoire *et al.*[13]

Comparing Figs. 3 and 6, one sees that despite a large change in γ, from 0.0 to 0.2, the size of discontinuity in S has hardly changed, which is rather surprising. There is, however, a reduction in the latent heat by a factor of about 2.5, as one can see from Table I, where the corresponding value for $\gamma=0.1$, from Brown,[8] is also given. The decrease in $\langle \Delta\varepsilon \rangle$ is more due to the cancellations between ΔC_{NN} and ΔC_{NNN} than due to individual decreases of either. In fact, this situation persists also at

TABLE I. Critical couplings for the phase boundaries in the three-dimensional three-state Potts model with antiferromagnetic next-nearest-neighbor coupling γ determined on a lattice of size L^3. Also given are the discontinuities in the nearest-neighbor (ΔC_{NN}) and the next-nearest-neighbor (ΔC_{NNN}) spin-spin expectation values, as well as the discontinuity in the average Hamiltonian per link, $\langle \Delta\varepsilon \rangle = 3\Delta(C_{\mathrm{NN}} - 2\gamma C_{\mathrm{NNN}})$. The first half of the table is for the order-disorder transitions, while the second half is for the order-order transition line between the two ordered phases with broken translation invariance. For the order-order transition line between the ferromagnetic and antiferromagnetic phases, we do not see any significant deviation from the classical prediction $\gamma_c=0.25$. Rows with asterisks indicate that the order of the transition could not be resolved.

β	γ	L	ΔC_{NN}	ΔC_{NNN}	$\langle \Delta\varepsilon \rangle$
0.55062(3)	0.0	∞	0.0533(23)		0.1599(69)
0.7417(3)	0.1	64	0.0494(23)	0.0650(31)	0.1092(87)
1.1901(1)	0.2	48	0.047(1)	0.066(1)	0.0618(42)
1.645(1)	0.24	32	0.054(1)	0.080(2)	0.0153(10)
1.822(2)	0.253	12	0.0063(11)	−0.1151(55)	0.1938(7)
1.806(1)	0.255	12	−0.0036(3)	−0.1509(15)	0.2202(6)
1.775(5)	0.26	12	0.0172(1)	−0.1260(6)	0.2481(15)
1.655(5)	0.3	12	0.0437(3)	−0.0454(2)	0.2127(12)
1.565(5)	0.35	20	0.0259(1)	−0.0254(1)	0.1311(3)
1.4805(5)	0.4	20	0.0142(4)	−0.0141(3)	0.0765(21)
1.410(5)	0.45	32	0.0106(1)	−0.0090(1)	0.0561(3)
1.317(3)	0.52	32	0.0049(1)	−0.0045(1)	0.0288(3)
1.222(3)	0.6	40	*	*	*
1.165(5)	0.65	40	*	*	*
1.0225(25)	0.8	40	*	*	*
1.185(5)	0.65	40	*	*	*
1.30	0.612(2)	20	−0.0009(3)	−0.0045(3)	0.0192(3)
1.40	0.593(2)	20	−0.0030(13)	−0.0077(13)	0.0186(6)
1.70	0.56(1)	12	−0.0102(10)	−0.0173(19)	0.0273(3)
2.00	0.543(1)	12	−0.0249(23)	−0.0304(32)	0.0243(6)

$\gamma=0.24$, where we had to simulate the model on lattices with $L \geq 32$ in order to obtain an estimate of $\langle \Delta\varepsilon \rangle$. A simulation in the critical regions $\beta=1.644$ and 1.645 on a 40^3 lattice clearly shows flips between two metastable states. Moreover, the size of the discontinuity in the order parameter S has remained unchanged compared with the smaller-γ values. Comparing with Fig. 4, one sees a significant increase in the fluctuations. However, apart from this quantitative difference, which is due to a decrease in $\langle \Delta\varepsilon \rangle$, one sees no qualitative change. In particular, C_{NN}, C_{NNN}, and other physical observables exhibit the same correlations in the flip-flop behavior. The disordered phase seems to be more probable at $\beta=1.644$, while the ordered one is so at $\beta=1.645$, suggesting that β_c lies in this interval.

In Table I we present the (β,γ) values of all transition points we investigated along with our estimates of corresponding discontinuities ΔC_{NN}, ΔC_{NNN}, and $\langle \Delta\varepsilon \rangle$. The results for the latent heat are presented also in Fig. 7, which shows that $\langle \Delta\varepsilon \rangle$ decreases approximately linearly as γ—the strength of the NNN antiferromagnetic coupling—increases in the interval $0 \leq \gamma \leq 0.24$. A linear extrapolation of the data to zero latent heat would suggest that this line of first-order phase transitions would terminate around $\gamma=0.3$. Thus the classical estimate of $\gamma_c=0.25$ can be realized only if a strong nonlinear behavior sets in in the interval [0.24,0.25]. In order to decide whether $\langle \Delta\varepsilon \rangle$ vanishes in the vicinity of $\gamma_c \simeq 0.25$ or stays finite requires a detailed study of the γ range between 0.24 and 0.25. Because of the increasing correlation length, related to the decrease in $\langle \Delta\varepsilon \rangle$, increasingly larger lattices will be needed in this region. A careful finite-size scaling analysis is thus called for. The possibility of nonvanishing $\langle \Delta\varepsilon \rangle$ gets further support from the analysis of the individual behavior of ΔC_{NN} and ΔC_{NNN}. In order for $\langle \Delta\varepsilon \rangle$ to be zero, either both ΔC_{NN} and ΔC_{NNN} should vanish or both should have the same sign, with the former being 2γ times the latter. Linear extrapolations using data for $\gamma \leq 0.24$ are suggestive of neither taking place near $\gamma=0.25$. Of course, it is possible that γ_c is greater than the classical expectation of 0.25. However, as our subsequent discussions of runs near $\gamma \sim 0.25$ will show, this cannot be the case.

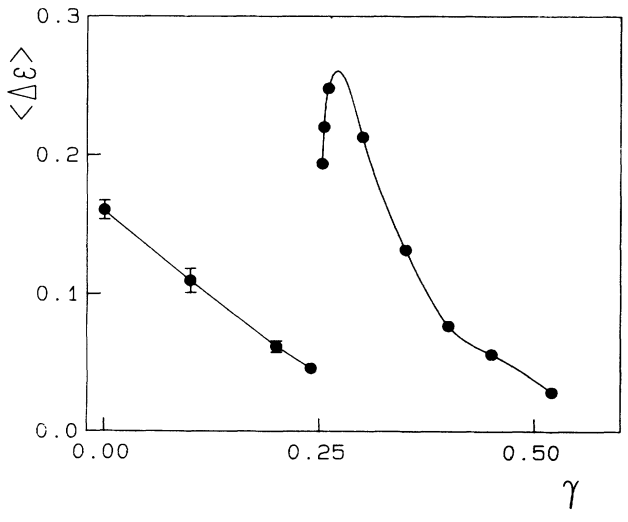

FIG. 7. Latent heat $\langle \Delta\varepsilon \rangle$ as a function of γ. The respective β_c and lattice sizes can be found in Table I.

In view of the expected phase diagram given in Fig. 2, we made several runs at $\gamma=0.25$ and $\beta=1.83$, 1.85, 1.86, and 1.9 on 12^3 lattices and in some cases on 16^3, 20^3, and 40^3 lattices. Figure 8 shows time evolutions of S for these runs on the 12^3 lattice. No structure is visible in the order parameter at $\beta=1.9$, while at $\beta=1.83$ one obtains large fluctuations; note that the scales are identical for all β values. A careful inspection reveals that $S_1 > S_2 = S_3$ for the entire run at $\beta=1.9$; i.e., the system is already in the SAF I phase. On the other hand, $\langle S_1 \rangle - \langle S_2 \rangle$ is rather small, being ~ 0.2, which indicates that only a few pairs of planes have acquired antiferromagnetic ordering. As β decreases from 1.9 to 1.86, already one finds a different behavior in the corresponding S evolution. Inspection of the $\bar{S}_\mu$'s in this case reveals that for this entire run also $\bar{S}_2=\bar{S}_3$, as shown in Fig. 9. The major difference, however, is the rich structure in Fig. 9, which was absent at $\beta=1.9$. It is even plausible that for a short time the lattice did go into the ferromagnetic phase in this run, where $\bar{S}_1=\bar{S}_2=\bar{S}_3$.

The intricate details of the structure are probably a reflection of the varying antiferromagnetic ordering pattern of the stack of the ferromagnetically ordered planes. Recall that the ground state in the SAF I phase has a degeneracy proportional to L, corresponding to possible antiferromagnetic orderings of the stack of ferromagnetic planes in one direction of the lattice. For sufficiently small lattices, one may expect the finite-size effects to permit the presence of some ferromagnetic ordering in the stack of the planes. Depending upon their amount, these impurities will cause the $\bar{S}_\mu$'s to change discontinuously. In fact, the different plateaus of $\bar{S}_2$ visible in Fig. 9 differ roughly by 0.125. Recalling the definition of $\bar{S}_2$ and $\bar{S}_3$ in Eqs. (6) and (7), it is easy to see that both will change by $3/2L^2L$ if one of the planes in the antiferromagnetically ordered stack of planes changes its internal ferromagnetic ordering [see also Fig. 1(c)]. On a 12^3 lattice, this works out to be 0.125. This discontinuity thus directly reflects the finite lattice extent and will probably shrink like $1/L$ in the infinite-volume limit. In addition to these runs, we performed simulations by changing γ from 0.248 to 0.252 and found a continuous increase in the number of planes ordered antiferromagnetically. The jumps between various orderings again appeared rather abrupt in $\bar{S}_\mu$ but smooth in bulk thermodynamic quantities such as ε.

Our study thus seems to suggest an absence of a sharp phase boundary between the ferromagnetic and SAF I phases, although a more detailed investigation on lattices of various sizes is perhaps necessary to clarify the nature of the phase boundary between the two ordered phases. It could, of course, be that one is dealing here with occurrences of metastable states corresponding to first-order phase transitions. But the lack of any associated structure in $\langle \varepsilon \rangle$ makes this rather improbable. As a concrete upshot of these runs, it seems one can rule out a γ_c

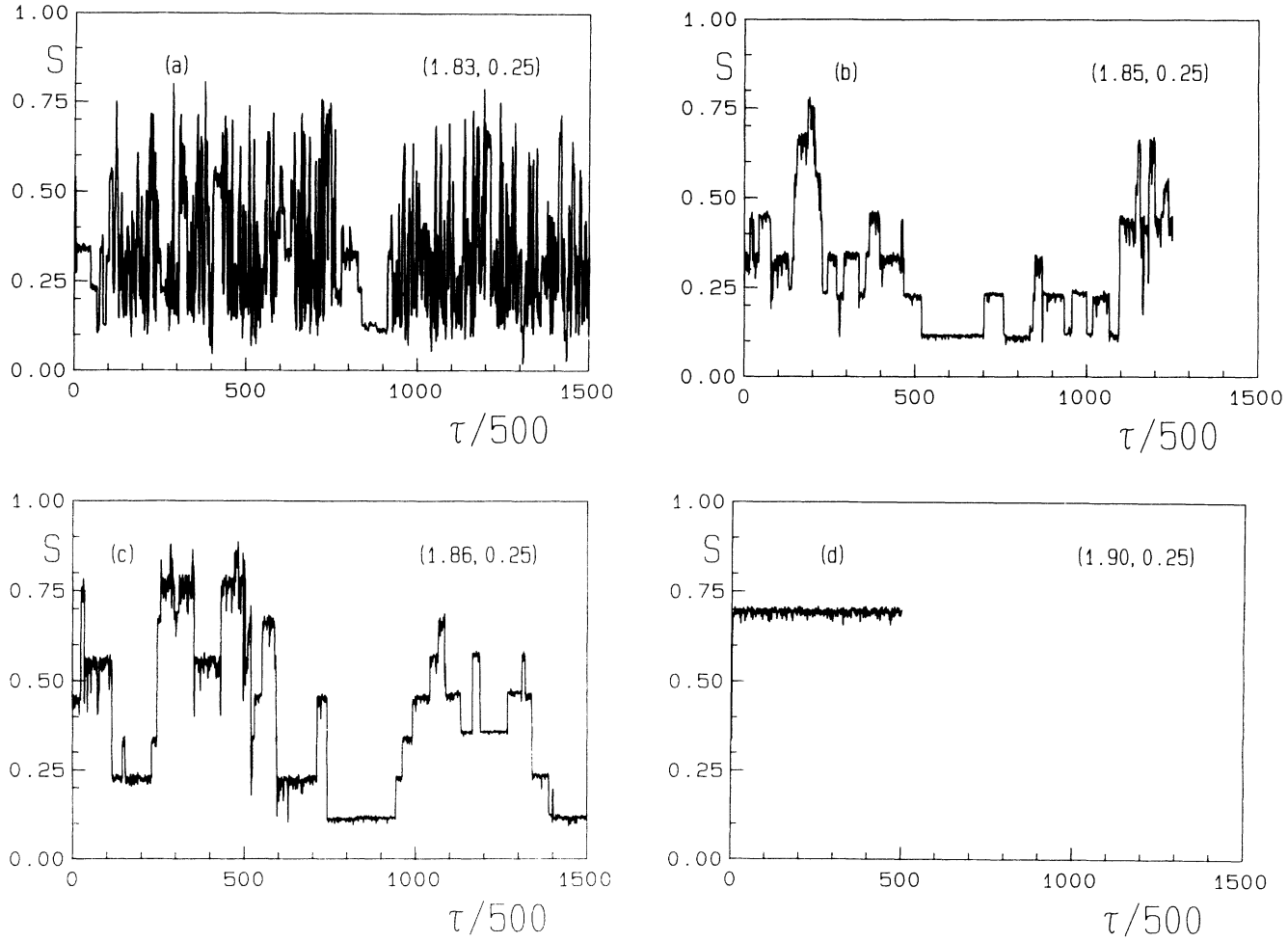

FIG. 8. Time evolution of the average spin S on a 12^3 lattice at $(\beta,\gamma)=$ (a) (1.83,0.25), (b) (1.85,0.25), (c) (1.86,0.25), and (d) (1.9,0.25).

larger than 0.25 since the SAF I phase appears to be present predominantly in all of them.

Any further detailed analysis of the nature of this tricritical point will require a special effort, including a detailed finite-size scaling analysis.[15] Recently, Lee and Kosterlitz have suggested a numerical method to distinguish a first-order phase transition from a second-order one which is useful for weak first-order phase transitions and has the potential of bringing out the tricritical nature.[16] However, it needs much more numerical work than we have been able to do since they use the Ferrenberg-Swendsen[17] method to extrapolate their MC data on various lattice sizes, but its use for two-coupling Hamiltonians such as ours in untested so far. One sees, nevertheless, that the nature of (1.86,0.25) can only be clarified by such techniques coupled with finite-size scaling analysis.

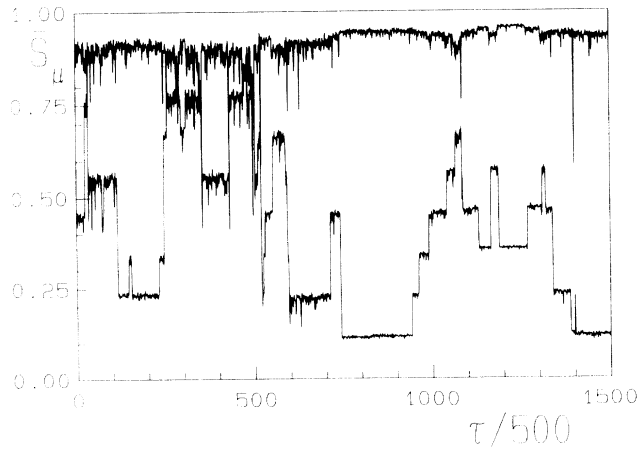

FIG. 9. Time evolution of $\bar{S}_\mu$, for $\mu=1,2$, on a 12^3 lattice at $(\beta,\gamma)=(1.86,0.25)$. For the entire run, $\bar{S}_2=\bar{S}_3$.

B. Superantiferromagnetic phase: $\gamma > 0.25$

Figure 10 shows the time evolution of S at $(\beta,\gamma)=(1.564,0.35)$ on a 16^3 lattice. A very clean flip-flop behavior between the ordered and disordered states is evident. In the ordered phase in this run, one finds $\langle \bar{S}_1 \rangle \sim 0.55$, whereas $\langle \bar{S}_2 \rangle \simeq \langle \bar{S}_3 \rangle \sim 0.11$. The latter values are indicative of an almost pure antiferromagnetic ordering of a stack of ferromagnetic planes. In the disor-

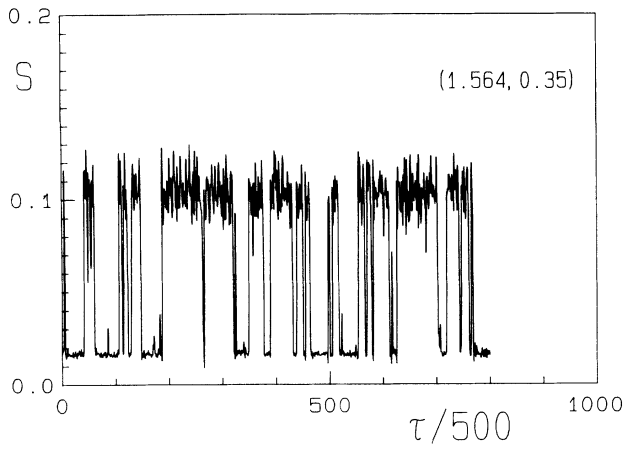

FIG. 10. Time evolution of the average spin S on a 16^3 lattice at $(\beta,\gamma)=(1.564,0.35)$.

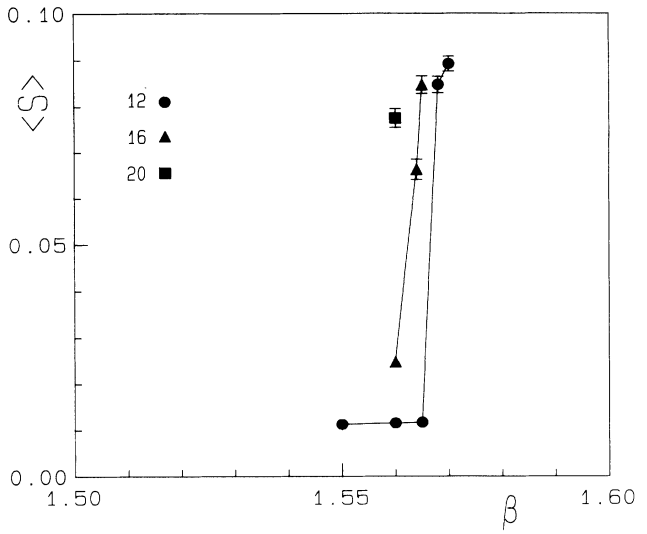

FIG. 11. Spin order parameter $\langle S\rangle$ as a function of β at $\gamma=0.35$ on L^3 lattices for $L=12$, 16, and 20.

dered phase, we found $\langle \bar{S}_1\rangle \simeq \langle \bar{S}_2\rangle \simeq \langle S_3\rangle \sim 0.1$. A detailed inspection of the time evolution of $C_{\rm NN}$ and $C_{\rm NNN}$ also reveals a behavior suggestive of jumps between two coexisting states. The interesting point, however, is that the $C_{\rm NNN}$ evolution is anticorrelated to that of $C_{\rm NN}$, ε, or S. This gives rise to a negative contribution to the latent heat, unlike in the disorder–ferromagnetic-order transitions for $\gamma<0.25$. Qualitatively, this is easily understood from the structure of the respective ground states. For $\beta\to 0$ the disordered state should have both $C_{\rm NN}\to\frac{1}{3}$ and $C_{\rm NNN}\to\frac{1}{3}$, while for $\beta\to\infty$ the ferromagnetically ordered state should have $C_{\rm NN}\to 1$ and $C_{\rm NNN}\to 1$, and the SAF I ordering should result in $C_{\rm NN}\to\frac{2}{3}$ and $C_{\rm NNN}\to\frac{1}{3}$. Of course, near β_c one expects the $\beta\to 0$ and $\beta\to\infty$ behavior to be lower and upper bounds, respectively, which imply $\Delta C_{\rm NN}\geq 0$, $\Delta C_{\rm NNN}\geq 0$ for the disorder–ferromagnetic-order phase transition, but $\Delta C_{\rm NN}\geq 0$, $\Delta C_{\rm NNN}\leq 0$ for the disorder–superantiferromagnetic-order transition. A more quantitative understanding of these gaps will naturally need high- and low-temperature expansions which will also be γ dependent. That the functional dependences on β and γ in these expansions are nontrivial can already be discerned from our Monte Carlo data.

Figures 11 and 12 show $\langle S\rangle$ and $\langle\varepsilon\rangle$ as a function of β for $\gamma=0.35$ on 12^3, 16^3, and 20^3 lattices. Once again, characteristic finite-size scaling features of a discontinuous transition are evident in these figures. Furthermore, β_c shifts to smaller values as the volume increases, and the shift is consistent with a V^{-1} behavior. Using the double-peak probability distributions, the data sample can be split into 2 and the estimates of $\Delta C_{\rm NN}$, $\Delta C_{\rm NNN}$, and $\langle\Delta\varepsilon\rangle$ so obtained from our largest lattice are given in Table I and Fig. 7. Note that individual values of $\Delta C_{\rm NN}$ and $\Delta C_{\rm NNN}$ in this case are a lot smaller than the corresponding values for $\gamma<0.25$, yet the negative sign of $\Delta C_{\rm NNN}$ gives rise to a sizeable latent heat.

We have made similar analyses at several values of $\gamma>0.25$. For the sake of brevity, we present the results only in a tabular form in Table I and Fig. 7, since these simulations display qualitatively the same features as those at $\gamma=0.35$ One sees some nontrivial and unexpected features in them. It seems that $\langle\Delta\varepsilon\rangle$ peaks at $\gamma=0.26$ and has a value which is ~ 1.5 times that at $\gamma=0.0$. Its major contribution comes from the $\Delta C_{\rm NNN}$ term. Both $\Delta C_{\rm NNN}$ and $\Delta C_{\rm NN}$ seem to reach their respective minimum around 0.255, where even the latter is negative. Again, a linear extrapolation of $\langle\Delta\varepsilon\rangle$ between 0.26 and 0.253, where it decreases, would reach zero at $\gamma\sim 0.23$. Of course, the data are much steeper here, and consequently such an extrapolation is more unreliable than the corresponding one for the data below $\gamma=0.25$. In particular, one notes a sharper decrease be-

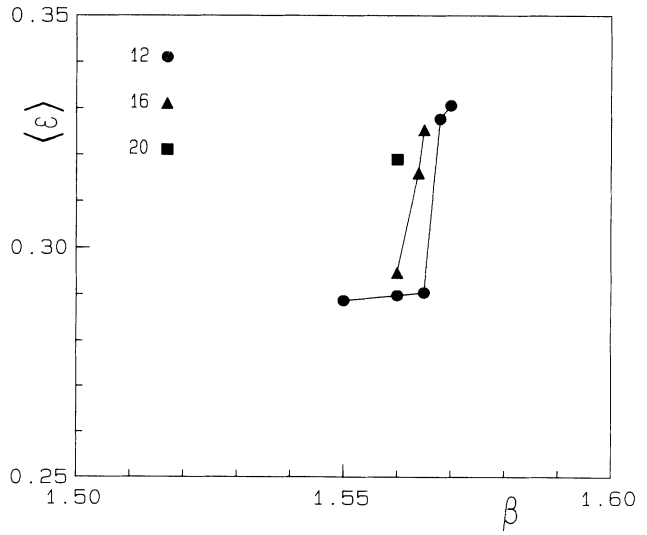

FIG. 12. Same as Fig. 11, but for the energy density $\langle\varepsilon\rangle$.

tween 0.255 and 0.253, suggesting that an even sharper decrease between $\gamma=0.253$ and 0.25, leading to $\langle \Delta\varepsilon \rangle = 0$ at $\gamma=0.25$, cannot be ruled out. Taking our estimates at face value, the trends in $\Delta C_{\rm NN}$ and $\Delta C_{\rm NNN}$ are, however, also not suggestive of $\langle \Delta\varepsilon \rangle$ vanishing at $\gamma=0.25$, since for that to happen either both should simultaneously vanish there or $\Delta C_{\rm NN} \simeq \Delta C_{\rm NNN}/2$. In conclusion, our simulations do not provide any evidence to suggest that $\langle \Delta\varepsilon \rangle = 0$ at $\gamma \simeq 0.25$, although it clearly does have a minimum in that neighborhood. Furthermore, $\Delta C_{\rm NNN}$ seems to have different signs on the two sides of the minimum; this coupled with the different behavior of the spin order parameter $\langle \bar{S}_\mu \rangle$ on these sides suggests that the transition region from ferromagnetic ordering to superantiferromagnetic ordering is, indeed, around $\gamma=0.25$, as classical minimum-energy criteria suggested. The precise location of the critical point in the γ interval [0.24,0.26] and investigations of its nature deserve a further more extensive investigation.

Considering now the region of $\gamma > 0.26$, one finds from Table I and Fig. 7 a monotonic decrease in $\langle \Delta\varepsilon \rangle$ as γ increases. It is noteworthy that $\Delta C_{\rm NN} \simeq -\Delta C_{\rm NNN}$ for $0.3 \le \gamma \le 0.52$, which is the largest γ up to which we could resolve a two-peak structure. The slow decrease in these observables taken together with the above approximate relation suggests that a vanishing $\langle \Delta\varepsilon \rangle$ will be obtained only at very large values of γ, i.e., for $\gamma \to \infty$. Clearly, with $\langle \Delta\varepsilon \rangle$ decreasing, one needs more and more statistics on larger and larger lattices to resolve a double-peak structure. Apart from this difference, however, one sees no qualitative change compared with the results at $\gamma=0.35$. For example, one always finds $\langle \bar{S}_2 \rangle \simeq \langle \bar{S}_3 \rangle < \langle \bar{S}_1 \rangle$ for the ordered phase, with $\langle \bar{S}_{2,3} \rangle \sim 0.1$. $\langle \bar{S}_1 \rangle$ decreases, however, continuously from ~ 0.9 at $\gamma=0.253$–0.255 to ~ 0.4 at $\gamma=0.4$, thus suggesting that the planes in the antiferromagnetically ordered stack are themselves dominantly ferromagnetic only for smaller γ values; for large γ, the NNN term distorts this ferromagnetic ordering significantly. This trend continues as γ increases, with a slight decrease in $\langle \bar{S}_2 \rangle = \langle \bar{S}_3 \rangle$, beyond $\gamma=0.5$. Recall that the classical considerations suggest the disorder-order phase transition to be between disordered and SAF II phase for $\gamma > 0.5$, and the latter should yield $\langle \bar{S}_1 \rangle \simeq \langle \bar{S}_2 \rangle$ with $\langle \bar{S}_3 \rangle$ smaller. At $\gamma=0.52$ we have, however, clear evidence that for $\beta=1.32$ and 1.33, which are just above our estimated $\beta_c = 1.317(3)$, $\langle \bar{S}_1 \rangle > \langle \bar{S}_2 \rangle \simeq \langle \bar{S}_3 \rangle$, and the phase transition appears to be discontinuous. For $0.52 < \gamma < 0.63$, the discontinuity, if present, is reduced to so low a value that we have been unable to estimate it properly even on a 40^3 lattice. However, the analysis of $\langle \bar{S}_\mu \rangle$, $\mu=1,2,3$, still suggests the ordered phase just above the disorder-order phase transition to be SAF I. For the multiphase point where the three phases SAF I, SAF II, and the disordered meet, we find

$$\gamma_c \simeq 0.63(2), \quad \beta_c = 1.18(2) . \tag{8}$$

C. Superantiferromagnetic II phase: $\gamma \ge 0.65$

As mentioned above, the SAF II phase can be identified by looking for the following behavior in the

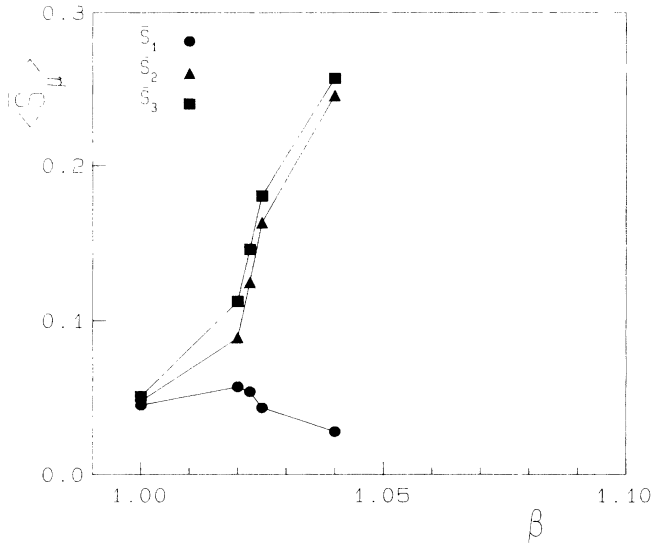

FIG. 13. $\langle \bar{S}_\mu \rangle$, $\mu=1,2,3$, as a function of β at $\gamma=0.8$ on a 40^3 lattice.

$\bar{S}_\mu$'s: $\langle \bar{S}_1 \rangle \simeq \langle \bar{S}_2 \rangle > \langle \bar{S}_3 \rangle$. Physically, the phase is characterized by a spontaneous breakdown of translational invariance in two directions: Ferromagnetic ordering persists only on lines parallel to the remaining direction, say, the z direction. It is easy to see then that planes perpendicular to the z direction will have an almost equal distribution of spins of each type, leading to $\langle \bar{S}_3 \rangle = O(1/L^2)$. On the other hand, both xz and yz planes will have an almost equal distribution of lines of ferromagnetically ordered spins, and hence $\langle \bar{S}_1 \rangle \simeq \langle \bar{S}_2 \rangle = O(1/L)$. Figures 13 and 14 demonstrate how these relations can be used to identify the boundaries between disordered, SAF I, and SAF II phases. Both exhibit $\bar{S}_\mu$, $\mu=1,2,3$. Figure 13 shows them as a function

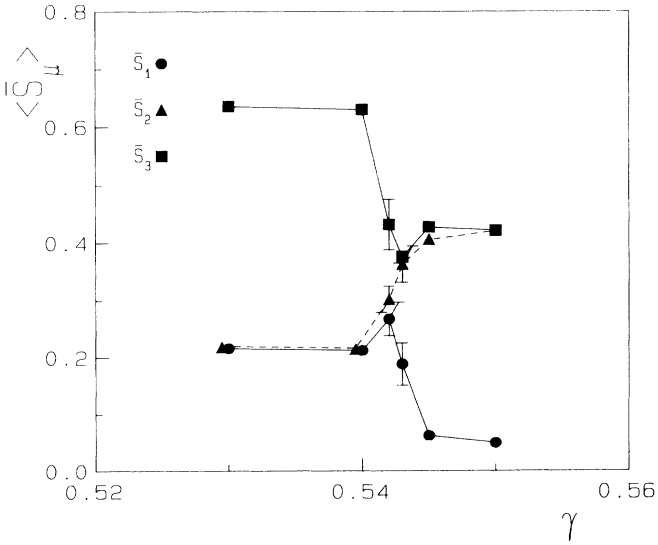

FIG. 14. $\langle \bar{S}_\mu \rangle$, $\mu=1,2,3$, as a function of γ at $\beta=2.0$ on a 12^3 lattice.

of β at $\gamma=0.8$ on a 40^3 lattice, while Fig. 14 shows $\bar{S}_\mu$ as a function of γ at $\beta=2.0$ on a 12^3 lattice. One sees that up to $\beta=1.022$ all $\bar{S}_\mu$'s are equal and small, while for $\beta \geq 1.03$, $\langle \bar{S}_1 \rangle = \langle \bar{S}_2 \rangle > \langle \bar{S}_3 \rangle$, suggesting that a transition from the disordered phase to the SAF II phase takes place at a β value in between. The corresponding energy density $\langle \varepsilon \rangle$, however, does not show any signs of a discontinuity. In view of our results for $\gamma < 0.65$, it is likely that the discontinuity, if present, is even smaller and therefore even more difficult to estimate than what was encountered there. The average spin $\langle S \rangle$, on the other hand, shows very little variation, which is to be expected since even in the ordered phase the population of each type of spin is roughly the same. We have repeated these simulations at $\gamma=0.65$ as well. Qualitatively, essentially the same picture emerges out of them, though identifying the critical region is complicated because of the proximity of the multiphase point where the three phase boundaries meet. Table I contains our estimates for β_c for these two cases. No definite statement about the order of the phase transition emerged out of our simulations. A study on larger lattices, coupled with finite-size scaling analysis, will be necessary to obtain a definitive result. It appears likely though that, as γ increases, $\langle \Delta\varepsilon \rangle \to 0$ asymptotically, as suggested by Fig. 7.

Turning to the phase boundary between the SAF I and SAF II phases, one sees from Fig. 14 that it is rather sharply defined for $\beta=2.0$. For $\gamma \leq 0.542$ one has $\langle \bar{S}_1 \rangle > \langle \bar{S}_2 \rangle = \langle \bar{S}_3 \rangle$, i.e., the SAF I phase, while for $\gamma \geq 0.543$, the data suggest the SAF II phase. The energy density $\langle \varepsilon \rangle$ shows almost no variation in this range of γ, but $\langle S \rangle$ changes rather rapidly. This is in accord with the expectations since $\langle S \rangle \sim O(L^{-2})$ for SAF II, but it should be between $O(1/L)$ and 0.25 for the SAF I phase, depending on how the antiferromagnetic ordering occurs.

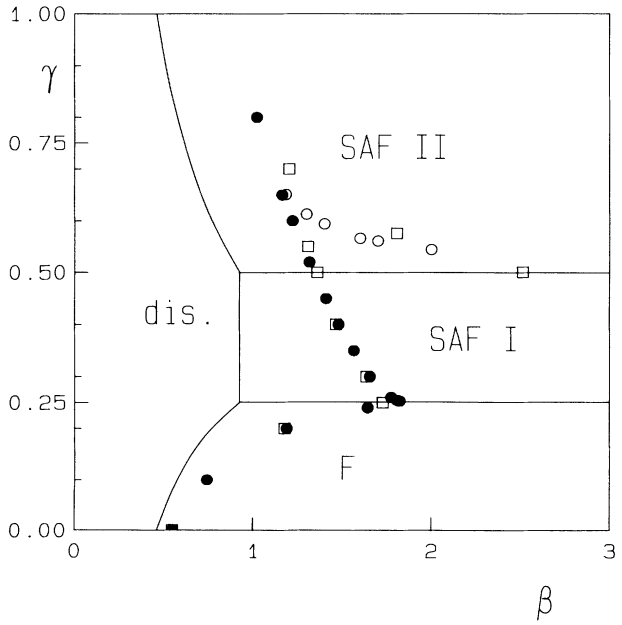

FIG. 15. Same as Fig. 2, but with our results on Monte Carlo simulations (circles) and those of Ref. 6 (squares).

Repeating this exercise at various β values, we obtained the phase boundary shown in Fig. 15. Along the entire phase boundary, we find, again qualitatively, the same behavior except that the boundary becomes less sharp as β decreases. Investigating the time histories of ε at the points on the boundary, one detects a small flip-flop structure, from which one can estimate the size of the discontinuity in $\langle \varepsilon \rangle$ along the boundary. Table I gives a summary of our results, which are separated from those corresponding to order-disorder phase transitions. Remembering the discussion in Sec. III C about the finite-size-induced changes in the energy density ε for degenerate vacua, it may be reemphasized that such effects may be present in this case too. In that case, though, $\langle \Delta\varepsilon \rangle$ will decrease as the lattice size increases. One can thus, in principle, check how genuine these discontinuities are.

IV. DISCUSSION AND CONCLUSIONS

The observed linear rise of the correlation length at T_c with the size of the lattice in the simulations of SU(3) gauge theory at finite temperatures, coupled with the universality arguments linking its critical behavior with that of three-dimensional spin models with $Z(3)$ global symmetry, rekindled interest in the issue of $Z(3)$ criticality or a lack thereof. In order to look for possible $Z(3)$ critical points, we simulated the three-dimensional three-state Potts model with nearest-neighbor (NN) ferromagnetic and next-nearest-neighbor (NNN) antiferromagnetic interaction on L^3 lattices for L ranging from 12 to 48. Using finite-size scaling techniques, as well as the appearance of qualitative signals such as characteristic flip-flop behavior, we obtained a phase diagram for this model shown in Fig. 15, where both the early numerical results[6] and a set of the theoretical expectations from Fig. 2 are also shown. In addition to the usual observables such as the average spin, we employed additional variables $\bar{S}_\mu$, defined in Eq. (7), to identify the physical nature of various phases. As one sees from Fig. 15, the classical and mean-field considerations yield a qualitatively correct phase diagram, but one also clearly sees their quantitative inadequacies, especially as γ increases. As discussed in Sec. II, the disorder-order phase transition lines for $\gamma > 0.25$ are guesses based on effective models. It would be interesting to compare a proper mean-field prediction for the full model with our data. We note that our results, obtained with better precision, are in broad agreement with those of Ref. 6, although near the triple-phase points we do have some differences.

Based on finite-size scaling analysis of global observables, we find a first-order phase transition along the order-disorder line for $0 \leq \gamma \leq 0.24$ and for $\gamma \geq 0.253$. From Fig. 7 one sees that the latent heat $\langle \Delta\varepsilon \rangle$ decreases almost linearly in the range $0 \leq \gamma \leq 0.24$, although ΔC_{NN} and $\langle \Delta S \rangle$ do not decrease in any substantial manner in this range. Any straightforward attempt at extrapolations, either direct or via ΔC_{NN} and ΔC_{NNN}, suggests a nonvanishing $\langle \Delta\varepsilon \rangle$ at $\gamma=0.25$. For $\gamma \geq 0.253$, $\langle \Delta\varepsilon \rangle$ first increases as ΔC_{NNN} acquires a negative sign. After peaking around $\gamma \simeq 0.26$, $\langle \Delta\varepsilon \rangle$ decreases continuously

with γ, with $\Delta C_{\mathrm{NN}} \simeq -\Delta C_{\mathrm{NNN}}$ for $0.3 \leq \gamma \leq 0.52$. This suggests that $\langle \Delta\varepsilon \rangle$ vanishes only for asymptotically large γ. While the decreasing latent heat necessitates larger lattices with greater statistics to establish a discontinuity, our analysis suggests that, except in the range $0.24 < \gamma < 0.253$, the order-disorder transition is first order, irrespective of the nature of the ordered phase. Even in the above γ range, a first-order phase transition is suggested, but the rapid changes of $\langle \Delta\varepsilon \rangle$ in that range render such a suggestion not so reliable. A more detailed finite-size study of this γ range is therefore called for.

For both the phase boundaries separating different ordered phases, our simulations suggest either a weak first-order line or no phase transition at all. Close to the boundaries, the lattice exhibits a mixture of the two orderings characteristic of the two phases separated by the boundary. Since changes in the energy density due to such mixtures are typically surface effects, one again needs to study $\langle \Delta\varepsilon \rangle$ along these boundaries as a function of lattice size in order to identify any genuine discontinuity that may exist. Perhaps, in the thermodynamic limit, a continuous range of different mixtures will be seen with no change in $\langle \varepsilon \rangle$, signaling that the boundary does not correspond to any sharp phase transition.

[1]H. W. J. Blöte and R. H. Swendsen, Phys. Rev. Lett. **43**, 799 (1979); S. J. Knak Jensen and O. J. Mouritsen, *ibid.* **43**, 1736 (1979).

[2]P. Bacielieri *et al.*, Phys. Rev. Lett. **61**, 1545 (1988); Nucl. Phys. **B318**, 553 (1989).

[3]J. Kogut *et al.*, Phys. Rev. Lett. **51**, 869 (1983); T. Celik, J. Engels, and H. Satz, Phys. Lett. **129B**, 323 (1983).

[4]A weak first-order phase transition was not ruled out.

[5]L. G. Yaffe and B. Svetitsky, Phys. Rev. D **26**, 963 (1982).

[6]S. Caracciolo and S. Patarnello, Phys. Lett. A **126**, 233 (1988).

[7]R. V. Gavai and F. Karsch, Pys. Lett. B **233**, 417 (1989); R. V. Gavai, in *Proceedings of Lattice 90, Capri, Italy,* edited by N. Cabibbo *et al.* [Nucl. Phys. B (PS) **17**, 335 (1990)].

[8]F. R. Brown, Phys. Lett. B **224**, 412 (1989); M. Bernaschi *et al.*, *ibid.* **231**, 157 (1989); A. Billoire, R. Lacaze, and A. Morel, Nucl. Phys. **B340**, 542 (1990); M. Fukugita, H. Mino, M. Okawa, and A. Ukawa, J. Stat. Phys. **59**, 1397 (1990).

[9]R. V. Gavai, F. Karsch, and B. Petersson, Nucl. Phys. **B322**, 738 (1989).

[10]Note that our β here is not the same as in Ref. 9. It is, in fact, 1.5 times the β used there. Also, Eq. (2.1) of Ref. 9 has a misprint: $-\beta$ in it should actually be $-\beta/2$.

[11]J. F. McCarthy (unpublished).

[12]We thank Professor M. M. Tsypin for suggesting this as a possible cause of the irregular behavior in $\beta_{c,L}$ reported in Ref. 7.

[13]A. Billoire, R. Lacaze, and A. Morel (Ref. 8).

[14]D. E. Knuth, *Seminumerical Algorithms,* 2nd ed., Vol. 2 of *The Art of Computer Programming* (Addison-Wesley, Reading, MA, 1973), Sec. 3.

[15]M. S. S. Challa, D. P. Landau, and K. Binder, Phys. Rev. B **34**, 1841 (1986).

[16]J. Lee and J. M. Kosterlitz, Phys. Rev. Lett. **65**, 137 (1990).

[17]A. M. Ferrenberg and R. H. Swendsen, Phys. Rev. Lett. **61**, 2635 (1988).

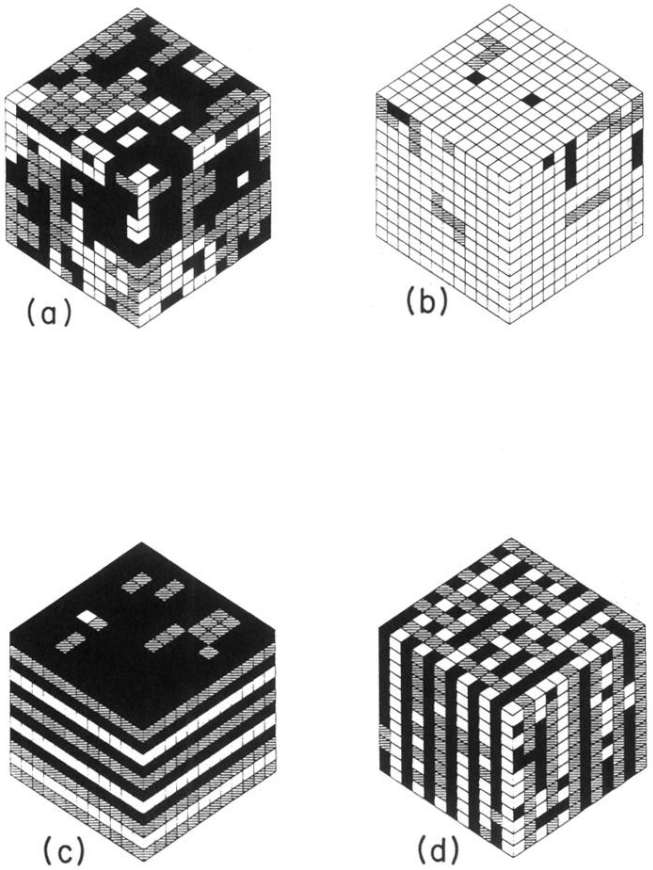

FIG. 1. Examples of typical configurations on a 12^3 lattice in the (a) disordered, (b) ferromagnetic, (c) type-I and (d) type-II superantiferromagnetic phases. The couplings used in these specific runs are $(\beta,\gamma)=$ (a) (1.805,0.255), (b) (1.645,0.24), (c) (1.807,0.255), and (d) (1.7,0.57).